On the failure of the quasicylindrical approximation and the connection to vortex breakdown in turbulent swirling flow

W. Gyllenram,[a] H. Nilsson, and L. Davidson
Division of Fluid Dynamics, Department of Applied Mechanics, Chalmers University of Technology,
SE-412 96 Gothenburg, Sweden

This paper analyzes the properties of viscous swirling flow in a pipe. The analysis is based on the time-averaged quasicylindrical Navier-Stokes equations and is applicable to steady, unsteady, and turbulent swirling flow. A method is developed to determine the critical level of swirl (vortex breakdown) for an arbitrary vortex. The method can also be used for an estimation of the radial velocity profile if the other components are given or measured along a single radial line. The quasicylindrical equations are rearranged to yield a single ordinary differential equation for the radial distribution of the radial velocity component. The equation is singular for certain levels of swirl. It is shown that the lowest swirl level at which the equation is singular corresponds exactly to the sufficient condition for axisymmetric vortex breakdown as derived by Wang and Rusak [J. Fluid Mech. **340**, 177 (1997)] and Rusak *et al.* [AIAA J. **36**, 1848 (1998)]. In narrow regions around the critical levels of swirl, the solution violates the quasicylindrical assumptions and the flow must undergo a drastic change of structure. The critical swirl level is determined by the sign change of the smallest eigenvalue of the discrete linear operator which relates the radial velocities to effects of viscosity and turbulence. It is shown that neither viscosity nor turbulence directly alters the critical level of swirl. © *2007 American Institute of Physics.* [DOI: 10.1063/1.2717724]

I. INTRODUCTION

Swirling flows are found in numerous applications. Turbines, compressors, and pumps all depend on the properties of swirling flow. For some applications, e.g., diffusers, a swirling velocity component may be introduced to stabilize the flow and to prevent separation. However, the stability of the flow can be completely lost if the swirl level is increased towards a certain limit, i.e., the swirl level at which a vortex breakdown may occur. A vortex breakdown often leads to a highly unsteady and turbulent flow that recirculates along its axis. In combuster applications, on the other hand, the turbulence and the recirculation zone are necessary to stabilize the burning flame. Beyond the complex interactions between the velocity components that arise from the presence of viscosity and turbulence, the governing equations are also unstable for other mathematical/physical reasons.

The stability of the axisymmetric incompressible Euler equations and its connection to vortex breakdown have been studied in numerous papers; see, for example, Benjamin,[1] Leibovich and Kribus,[2] Szeri and Holmes,[3] and Wang and Rusak.[4] In these papers, the equations are transformed to either the Squire-Long (Bragg-Hawthorne) equation or to the equations derived by Szeri and Holmes.[3] The assumption of radial equilibrium is often a part of the analysis[1,3,4] as it describes the class of *columnar flows* in which the radial velocity component is zero and there are no axial gradients. If the flow field is not homogeneous in the axial direction, the assumption of radial equilibrium is taken locally.[2] As

Szeri and Holmes[3] pointed out, *any* combination of axial and tangential velocities will in this case be a solution to the Euler and continuity equations, i.e., the velocity components are independent.

The radial velocity component is usually not measured in swirling flow because of its low magnitude and other practical reasons, such as visual access. Numericists who use measured data as inlet boundary conditions then lack some information about the flow field, which is of course unsatisfactory. Many times the radial velocity is neglected at the inlet boundary, as in the numerical studies of axisymmetric vortex breakdown by Brown and Lopez,[5] Beran and Culick,[6] and Lopez.[7] However, as will be shown in Sec. III, radial velocities are a direct consequence of viscosity and/or turbulence and their magnitudes may be significant for low Reynolds numbers. It will also be shown how an estimation of the radial velocity component in steady flow can be obtained if the two other components are known along a single radius. An analytical estimation of the radial velocity in the case that the other components are given is of interest to both experimentalists and numericists. If the radial velocity component of a low Reynolds number swirling flow is neglected at the inlet boundary of a simulation, it is possible that the near downstream flow may be forced to a columnar state that is unphysical.

Benjamin[1] introduced the concept of subcritical and supercritical states of a swirling flow by analogy with the hydraulic jump. By introducing perturbations to the Squire-Long equation, the stability of the flow was analyzed as an eigenvalue problem. He analyzed the sign of the smallest eigenvalue for a given perturbation to a given columnar flow field and showed that disturbances to the flow field may

[a]Author to whom correspondence should be addressed. Electronic mail: gyllwalt@chalmers.se

propagate upstream only if the swirl level reaches a certain value. At this point, the smallest eigenvalue of the problem must become negative. If the swirl level is higher than critical, the state of flow is referred to as the subcritical state. The existence of these states has been verified by Wang and Rusak,[4] who analyzed the stability of the disturbances in a forced vortex (solid body rotation) in a pipe and found that the disturbance is stable in the subcritical state and unstable in the supercritical state. The instability of the disturbance in the supercritical state is explained by the washout effect of the axial flow, which will be of greater magnitude than the upstream propagation speed of the disturbance. If a disturbance turns out to be stable, it is proposed that it will lead to vortex breakdown. Wang and Rusak[8,9] introduced the effects of slight viscosity in their analysis of the Szeri-Holmes equation and made an extensive analysis of the time-asymptotic behavior of the flow. Rusak et al.[10] extended this analysis and derived necessary and sufficient conditions for the axisymmetric vortex breakdown of a q vortex in a pipe, of which the latter corresponds to the critical swirl level of Benjamin.[1] The results are extended in Rusak and Judd[11] to include swirling flows in diverging stream tubes.

The breakdown of viscous swirling flows was numerically analyzed by Hall[12] and Bossel,[13] who both examined the failure of the quasicylindrical approximation of the Navier-Stokes equations. Bossel[14,15] also used the quasicylindrical approximation for the outer viscous field of a vortex core and inviscid equations for the flow close to the axis. Brown and Lopez[5] used the Navier-Stokes equations to numerically analyze a laminar axisymmetric swirling flow in a pipe. They argue that the physical mechanism behind a vortex breakdown rely on the production of a negative azimuthal component of vorticity. In fact, since $\omega_\theta \sim -\partial_r V_z$, this is equivalent to a deceleration of the axial velocity at the centerline, which often is observed in studies of vortex breakdown. A more recent paper by Lopez[7] discusses the stability of laminar swirling flow subject to an axisymmetric disturbance. Lopez solves the axisymmetric Navier-Stokes equations at low Reynolds numbers, but neglects the effects of boundary layers. Lopez finds a critical level of swirl that is very close to the sufficient condition for vortex breakdown derived by Rusak et al.[10] Both steady and unsteady solutions were analyzed. The steady solutions confirm the results obtained by Beran and Culick[6] for the same case. It is clear that there is a range of swirl levels for which multiple solutions to the axisymmetric Navier-stokes equations exist. Lopez[7] also showed that the steady solutions and time averages of unsteady solutions do not coincide. Beran[16] extended the results of Beran and Culick[6] to include unsteady solutions to the problem and found that every unsteady solution asymptotically reaches steady state and coincides with the solutions to the steady equations, i.e., no stable unsteady solution branch is found, as in the work of Lopez.[7] However, the time-asymptotic solutions were very sensitive to the initial conditions, which confirms that there is a range of swirl levels for which multiple solutions can exist. In Beran and Culick,[6] also the behavior of the quasicylindrical equations is investigated. They found that the quasicylindrical method provided an efficient approximation for the critical level of

swirl. The quasicylindrical approach was, however, criticized by Lopez,[7] who argues that this method is incapable of describing the evolution of any flow approaching vortex breakdown and fails at much lower swirl levels than those needed for the flow to stagnate. Indeed, the equations can never describe the nonlinear physics of a vortex breakdown near a stagnation point. However, as also mentioned by Lopez, "a vortex should not be classified as having undergone breakdown based on the stagnation of its axial flow." As will be shown in this paper, the failure of the quasicylindrical equations occurs at exactly the same swirl level which determines the sufficient condition for vortex breakdown as derived by Wang and Rusak[9] and Rusak et al.,[10] and shown by Lopez.[7] The reason why Hall[12] and Beran and Culick[6] did not reach this critical swirl level may be explained by the iterative stepping methods that were used. Any iterative method will fail when the problem gets ill conditioned, as in the region around a singularity.

Vortex breakdown has obviously been the subject of many studies, and there are still several definitions of what it actually is. However, it is most commonly agreed upon to be a sudden change in flow structure of a vortical flow, most often connected to a deceleration of the axial flow in the vortex core. Experimental visualizations of vortex breakdown in laminar flows by Mattner et al.[17] and Sotiropoulos and Ventikos[18] have shown structures reminiscent of bubbles, which are approached by the surrounded flow field as if they were solid obstacles. Snyder and Spall[19] numerically reproduced the bubble-type vortex breakdown that was found experimentally by Sarpkaya.[20] The breakdown into steady or unsteady spiral shapes, which is very common in turbulent flow, has also been investigated (see Alekseenko et al.[21]).

The analysis provided herein may in some sense be regarded as a link between the theories of Hall[12,22] and Benjamin[1] as it connects the failure of the quasicylindrical Navier-Stokes equations to the sign change of the smallest eigenvalue of the system. The time-averaged quasicylindrical Navier-Stokes equations are derived and analyzed in Sec. II. The equations are rearranged to yield a single linear differential equation for the radial distribution of the radial velocity component. The critical swirl level is determined by the properties of the linear operator that relates the radial velocities to effects of viscosity and turbulence. The singularities of the equation are found by an exact numerical method, and the results show that the singularities of the quasicylindrical equations correspond exactly to the critical swirl levels found by Wang and Rusak,[9] Rusak et al.,[10] and Lopez.[7]

II. DERIVATION OF A LINEAR EQUATION FOR THE RADIAL VELOCITY COMPONENT

Vortex breakdown is generally unsteady and asymmetric. Nevertheless, a time-averaged flow field will be axisymmetric in any axisymmetric domain. Furthermore, the time-averaged radial velocities of an unsteady helicoidal swirling flow may be considered small even if the instantaneous flow field has significant radial velocities locally. A time average will be equivalent to a tangential average if the unsteady

helicoidal flow is periodic, and a sign change of the radial velocity component in the tangential direction will lead to a small value in mean. Hence, a quasicylindrical approach based on the time-averaged Navier-Stokes equations can in some sense be considered more general than using the axisymmetric Navier-Stokes equations directly.

It is shown in the Appendix that a second-order approximation of the time-averaged Navier-Stokes equations for turbulent swirling flow in a straight (or slightly diverging) pipe read

$$-\frac{1}{r}V_\theta^2 = -\frac{1}{\rho}\partial_r P, \tag{1}$$

$$V_r\partial_r V_\theta + V_z\partial_z V_\theta + \frac{1}{r}V_r V_\theta = -\frac{1}{r}\partial_r(r\overline{v_r'v_\theta'}) - \frac{1}{r}(\overline{v_r'v_\theta'}), \tag{2}$$

$$V_r\partial_r V_z + V_z\partial_z V_z = -\frac{1}{\rho}\partial_z P - \frac{1}{r}\partial_r(r\overline{v_r'v_z'}), \tag{3}$$

and, for steady flow $(100 < \mathrm{Re} < 1000)$, we have

$$-\frac{1}{r}V_\theta^2 = -\frac{1}{\rho}\partial_r P, \tag{4}$$

$$V_r\partial_r V_\theta + V_z\partial_z V_\theta + \frac{1}{r}V_r V_\theta = \frac{1}{r}\partial_r(\nu r\partial_r V_\theta) - \frac{1}{r}\left(\nu\frac{V_\theta}{r}\right), \tag{5}$$

$$V_r\partial_r V_z + V_z\partial_z V_z = -\frac{1}{\rho}\partial_z P + \frac{1}{r}\partial_r(\nu r\partial_r V_z), \tag{6}$$

and the corresponding continuity equation is

$$\frac{1}{r}\partial_r(rV_r) + \partial_z V_z = 0. \tag{7}$$

If the tangential and axial velocity profiles are prescribed, an expression for the radial component can be derived. Taking the radial gradient of the axial momentum equation (3) and using the continuity equation (7) gives

$$\partial_r(V_r\partial_r V_z) - \partial_r\left(\frac{V_z}{r}\partial_r(rV_r)\right) = -\frac{1}{\rho}\partial_r\partial_z P$$

$$-\partial_r\left(\frac{1}{r}\partial_r(r\overline{v_r'v_z'})\right). \tag{8}$$

The radial momentum equation (1) can be derivated in the axial direction to yield

$$-\frac{1}{\rho}\partial_z\partial_r P = -\frac{2}{r}V_\theta\partial_z V_\theta, \tag{9}$$

and the tangential momentum equation (2) can be expressed as

$$\partial_z V_\theta = -\frac{1}{V_z}\left[\frac{1}{r}\partial_r(r\overline{v_r'v_\theta'}) + \frac{1}{r}(\overline{v_r'v_\theta'}) + V_r\partial_r V_\theta + \frac{1}{r}V_r V_\theta\right]. \tag{10}$$

If this expression of the tangential momentum equation is inserted into Eq. (9) we get

$$-\frac{1}{\rho}\partial_z\partial_r P = \frac{2V_\theta}{rV_z}\left[\frac{1}{r}\partial_r(r\overline{v_r'v_\theta'}) + \frac{1}{r}(\overline{v_r'v_\theta'}) + V_r\partial_r V_\theta \right.$$

$$\left. + \frac{1}{r}V_r V_\theta\right], \tag{11}$$

which in turn can replace the pressure term in the axial momentum equation (8) to yield

$$\partial_r(V_r\partial_r V_z) - \partial_r\left(\frac{V_z}{r}\partial_r(rV_r)\right) = \frac{2V_\theta}{rV_z}\left[\frac{1}{r}\partial_r(r\overline{v_r'v_\theta'}) + \frac{1}{r}(\overline{v_r'v_\theta'}) \right.$$

$$\left. + V_r\partial_r V_\theta + \frac{1}{r}V_r V_\theta\right]$$

$$-\partial_r\left(\frac{1}{r}\partial_r(r\overline{v_r'v_z'})\right). \tag{12}$$

The left-hand side of Eq. (12) can be rewritten as

$$\partial_r(V_r\partial_r V_z) - \partial_r\left(\frac{V_z}{r}\partial_r(rV_r)\right) = V_r\partial_r\partial_r V_z - V_r\partial_r\frac{V_z}{r} - \frac{V_z}{r}\partial_r V_r$$

$$- V_z\partial_r\partial_r V_r, \tag{13}$$

and, after some manipulation, a second-order linear differential equation for V_r can be obtained, i.e.,

$$f\partial_r\partial_r V_r + g\partial_r V_r + h V_r = b, \tag{14}$$

where the coefficients are defined as

$$f(V_z(r,z)) = -V_z, \tag{15}$$

$$g(V_z(r,z),r) = -\frac{V_z}{r}, \tag{16}$$

$$h(V_\theta(r,z),V_z(r,z),r) = \partial_r\partial_r V_z + \frac{V_z}{r^2} - \frac{\partial_r V_z}{r} - \frac{2V_\theta^2}{r^2 V_z}$$

$$- \frac{2V_\theta\partial_r V_\theta}{rV_z}, \tag{17}$$

and

$$b(V_\theta(r,z),V_z(r,z),r,\cdot') = \frac{2V_\theta}{rV_z}\left[\frac{1}{r}\partial_r(r\overline{v_r'v_\theta'}) + \frac{1}{r}(\overline{v_r'v_\theta'})\right]$$

$$-\partial_r\left(\frac{1}{r}\partial_r(r\overline{v_r'v_z'})\right). \tag{18}$$

Symbol $\cdot'$ in the parentheses after coefficient b denotes the dependence on turbulence or unsteadiness. For the steady case, only source term b will have to be modified, i.e.,

$$b_{st}(V_\theta(r,z),V_z(r,z),r) = -\frac{2V_\theta}{rV_z}\left[\frac{1}{r}\partial_r(\nu r\partial_r V_\theta) - \frac{1}{r}\left(\nu\frac{V_\theta}{r}\right)\right]$$

$$+\partial_r\left(\frac{1}{r}\partial_r(\nu r\partial_r V_z)\right). \tag{19}$$

For a steady case, Eq. (14) can now be solved for any combination of V_z and V_θ to give a corresponding radial velocity component. The result will, however, only be useful if it is of the same order of magnitude as was assumed.

The appropriate boundary conditions for V_r read

$$V_r|_{r=0} = V_r|_{r=R} = 0. \qquad (20)$$

The above relations assure symmetry at the centerline and fulfill the necessary kinematic boundary condition for a (nonporous) wall, thus closing the system. Equation (14) can be discretized and written as

$$A\mathbf{v} = \mathbf{s}. \qquad (21)$$

The coefficients of matrix A are discrete functions of the axial and tangential velocity profiles, the elements of vector $\mathbf{v}$ describe the radial distribution of the radial velocity component, and vector $\mathbf{s}$ is the integrated form of the source term, Eqs. (18) and (19). See the Appendix for details about the discretization and solution method.

III. RESULTS AND DISCUSSION

A few conclusions can be directly drawn from the form of Eq. (14). If the flow is steady and inviscid, $V_r=0$ because of the vanishing source term b_{st}, Eq. (19), and the boundary conditions (20). This can be mathematically proven by the weak maximum principle,[23] but it is rather obvious from Eq. (14). If we insert a uniform axial velocity profile and a solid body rotation the source term, b_{st}, will vanish independent of the Reynolds number, and the solution to Eq. (14) is again $V_r=0$. However, it will be shown in the following sections that there exist critical swirl levels for which the matrix A in Eq. (21) is not invertible. For these swirl levels there exist no solutions to Eq. (14).

A. Determination of supercritical and subcritical regions of an arbitrary vortex

To determine whether supercritical and subcritical states exist for a quasicylindrical flow, the eigenvalues of the discrete linear operator A in Eq. (21) are analyzed. No knowledge of turbulence or viscous terms is needed for this analysis as they are not part of matrix A. Simple polynomial or exponential functions for the axial and tangential velocities are used throughout this work. The method is nevertheless applicable for arbitrary vortices. As a start, we define a set of axial and tangential velocity profiles as

$$V_z = U_0(4r^2/R^2 - 5r^3/R^3 + 1), \qquad (22)$$

$$V_\theta = U_\theta \sin(\pi r/R). \qquad (23)$$

These profiles are chosen because they resemble a typical vortex often found experimentally, as in Dellenback et al.[24] With the exception of the boundary layers, this combination of axial and tangential velocity profiles somewhat resembles a q vortex (see Sec. III B). The axial velocity profile fulfills the necessary Neumann condition at $r=0$, where it has a local minimum, and a no-slip boundary condition at $r=R$. The low order of the polynomial reduces the discretization errors to a minimum. The bulk velocity, U_0, is used as a scaling parameter. The form of the tangential velocity fulfills the necessary boundary conditions, and the maximum tangential velocity, U_θ, is used as a scaling parameter. In analyzing different swirl numbers, the relation between the maximum tangential velocity and the bulk velocity should be
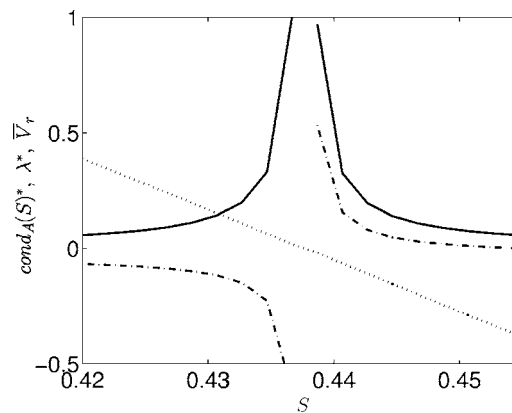

FIG. 1. Properties of matrix A for steady swirling flow at Re$=100$ over swirl number S. The swirl is varied by increasing the coefficient U_θ of Eq. (23). [$\cdot\cdot$] The smallest eigenvalue of matrix A, i.e., λ^* $=\min\{\lambda\}/(R^{-2}\int_R \mathbf{V}^2/2rdr)$; (-) the condition number of matrix A, i.e., $\text{cond}_A(S)^* = \text{cond}_A(S)/\max\{\text{cond}_A(S)\}$; (--) computed and averaged radial velocity from Eq. (14), i.e., $\bar{V}_r(S)=R^{-2}\int_R V_r/U_0 rdr$.

of the order of 1, i.e., $U_\theta/U_0 \sim 1$. The swirl number is here defined as

$$S \equiv \frac{1}{R} \frac{\int_0^R V_z V_\theta r^2 dr}{\int_0^R V_z^2 rdr} \qquad (24)$$

and relates the flux of angular momentum to the flux of axial momentum. The condition number of A as a function of swirl number is shown in Fig. 1. As one eigenvalue approaches zero, the condition number approaches infinity and the (radially averaged) radial velocity approaches $+/-$ infinity, depending on the sign of the smallest eigenvalue. Once one of the eigenvalues approaches zero, the flow must undergo a drastic change in structure as the quasicylindrical approximation will not hold, i.e., Eq. (14) will be singular. At swirl levels $S>S_{\text{crit}}$ the quasicylindrical approximation is again valid and a near columnar flow may exist. The possible existence of near columnar flow at subcritical swirl levels has earlier been suggested by Wang and Rusak[9] and is confirmed by the (time-averaged) experimental results of Dellenback et al.[24] By further increasing the swirl number, Eq. (14) will have other singular points as all positive eigenvalues will decrease and eventually approach zero. This property was also found by Bossel,[13] who analyzed the two-dimensional solution to the quasicylindrical equations by the method of weighted residuals. Bossel found an infinite set of singularities. Obviously, for the present discretized case, the number of singularities is directly linked to the size of the computational grid. Since the equations are derived under the assumption that $V_\theta \sim V_z$, solutions for very large swirl numbers cannot be trusted. Consequently, only the first few singular points will have a physical meaning. With a refinement of the grid, all eigenvalues will be influenced. However, the critical swirl number is not influenced by the grid resolution, as is shown in Fig. 2. Since the magnitude of the critical swirl number is apparently independent of resolution, it is sug-
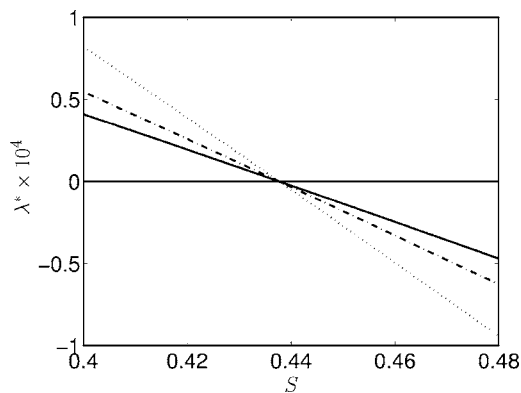
FIG. 2. The smallest eigenvalue, λ^*, of the discrete operator A as a function of swirl number S, calculated at three different resolutions: $(\cdot\cdot)$ 200, $(\cdot\text{-})$ 300, (-) and 400 nodes.

gested that the critical point is connected to the axis of the vortex core. Close to the symmetry axis, at small r/R, the axial velocity profile is constant and the tangential velocity profile is approximately linear. Hence, if a second-order numerical scheme is used, the resolution is in this limit not decisive for a proper representation of the coefficients of Eq. (14).

One eigenvalue is negative in the subcritical swirl region. From Fig. 3, which presents solutions to Eq. (14) for steady flow, it can be concluded that the existence of a quasicylindrical flow is also possible for swirl numbers above critical. Another very interesting property of the subcritical flow is shown in Fig. 3 (top). When $S > S_{\text{crit}}$, but is not too large, both the radial velocity and (consequently) its radial derivative are positive in the core region ($r/R \lesssim 0.5$). It follows from the continuity equation (7) that

$$\partial_z V_z < 0, \tag{25}$$

and it is obvious that, for this special vortex, the slightly subcritical state must lead to a deceleration of the axial flow in the vortex core. This behavior of the vortex at swirl levels close to critical is by no means universal, as will be shown in Sec. III C. The critical swirl level of a vortex is determined by its axial and tangential velocity profiles. Moreover, the behavior of the vortex near this critical level is also determined by the distributions of the axial and tangential velocities.

B. Critical swirl level of a *q* vortex

In this section a q vortex[7,10] is studied. The axial and tangential velocity profiles of the vortex can be defined as

$$V_z = V_0 + V_1 e^{-r^2/R_c^2}, \tag{26}$$

$$V_\theta = \Omega R_c^2 (1 - e^{-r^2/R_c^2})/r. \tag{27}$$

The shape of the velocity profiles are determined by four parameters: V_0, V_1, R_c, and Ω. The sum of V_0 and V_1 defines the centerline velocity and R_c is proportional to the radius of the vortex core, i.e., the radius at which the tangential velocity has its maximum. For a q vortex $r_c = 1.12 \times R_c$. Ω is the angular velocity of the vortex core. The q vortex does not
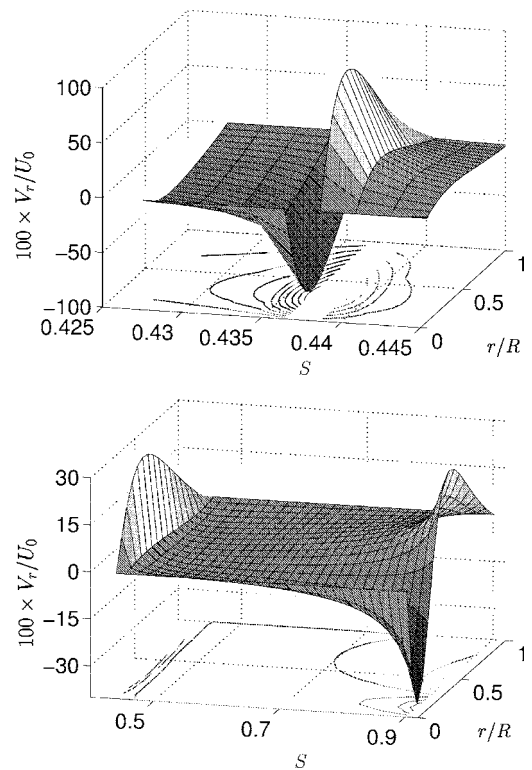

FIG. 3. The radial velocity component in steady flow around the critical swirl number, S_{crit}, computed from Eq. (14) at Re = 100. The swirl is varied by increasing coefficient U_θ of Eq. (23). Top: The results violate the quasicylindrical assumptions in the near critical region because it is assumed that $100 \times V_r/U_0 \lesssim 1$. With a finer resolution in the S dimension, the radial velocities would approach $(-/+)$ infinity at the critical level. Bottom: In narrow regions around the first and second critical swirl numbers, the results violate the quasicylindrical assumptions. The tendency of flow deceleration along the axis of symmetry appears only in the slightly subcritical region.

fulfill the no-slip boundary condition at $r = R$. Hence, the boundary layers are neglected. First, we analyze $V_1 = \pm V_0/4$ using various ratios of R_c/R. For each case, the swirl level is varied by letting the radius of the domain increase while the axial mass flow, the flux of angular momentum, and the ratio R_c/R are kept constant. As the axial velocity decreases quadratically with an increase in radius, the swirl number will, according to Eq. (24), increase linearly. For each case, the radius is increased until the first singularity of matrix A in Eq. (21) is found.

Three definitions of a swirl number have been used, i.e., the integral form, Eq. (24), and two local forms,

$$S_c \equiv \max(V_\theta)/V_z|_{r=0}, \tag{28}$$

$$S_\phi \equiv \max(V_\theta/V_z), \tag{29}$$

of which the latter can be interpreted as the (tangents of) maximum swirl angle. An analytical expression for the maximum tangential velocity of a q vortex reads[10] $\max(V_\theta) = 0.638 \times \Omega R_c$, which gives $S_c = 0.638 \times \Omega R_c/(V_0 + V_1)$. The results are shown in Fig. 4. It is clear that none of the definitions of swirl number gives a constant value for the level of vortex breakdown. However, the larger a vortex core radius, the higher a level of critical swirl.
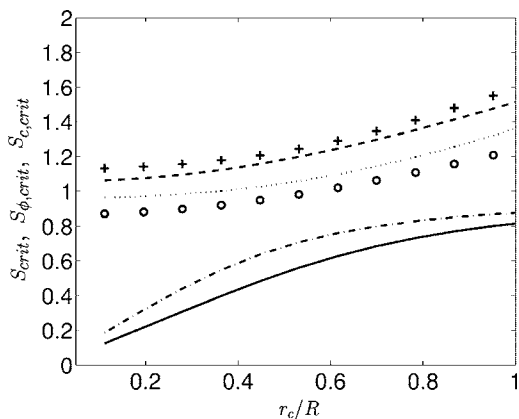
FIG. 4. The critical swirl levels of two q vortices as a function of the vortex core radius. (+) The maximum swirl angle S_ϕ, calculated from Eq. (29), $V_1=0.25$; (·) same as previous, except $V_1=-0.25$. (··) The swirl number S_c, calculated from Eq. (28), $V_1=0.25$; (--) same as the previous, except $V_1=-0.25$. (-·-) The integral swirl number S, calculated from Eq. (24), $V_1=0.25$; (-) same as previous, except $V_1=-0.25$.

Figure 5 shows the critical swirl number, $S_{c,\text{crit}}$, as a function of the vortex core radius for two other q vortices, $V_1/V_0=1$ (top) and $V_1/V_0=-0.5$ (bottom). It is obvious that the critical level of swirl predicted by the method derived in this paper is identical to the sufficient condition for axisymmetric vortex breakdown derived by Rusak *et al.*[10] This
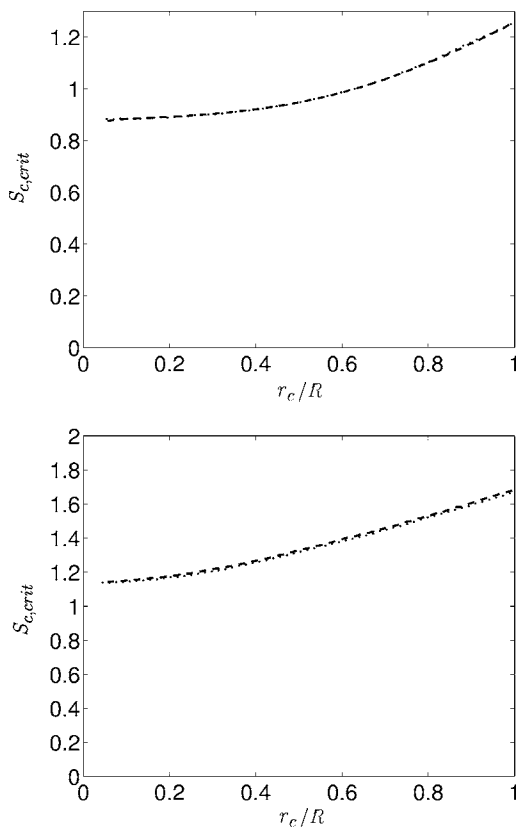

FIG. 5. The critical swirl level $S_{c,\text{crit}}$ as a function of the vortex core radius for two q vortices. (--) The critical swirl level corresponding to the first singular point of the quasicylindrical equations; (·) the sufficient level of swirl for axisymmetric vortex breakdown derived by Rusak *et al.* (Ref. 10). Top: $V_1/V_0=1$. Bottom: $V_1/V_0=-0.5$. The results are identical.

TABLE I. The (nondimensional) critical swirl level $\omega_B=\Omega R_c^2/(V_0 R)$ of a Burgers vortex at various Reynolds numbers. All methods predict nearly the same, or identical, level of critical swirl.

Reference	Re	ω_B
Wang and Rusak (Ref. 9)	∞	0.8829
Lopez (Ref. 7)	1000	0.9
Present	Any	0.8829

shows that the first singularity of the quasicylindrical equations corresponds exactly to the global minimizer solution of Rusak *et al.*[10]

C. Critical swirl level of a Burgers vortex

A Burgers vortex is a special case of the q vortex, Eqs. (26) and (27), in which $V_1=0$. Wang and Rusak[9] calculated the critical swirl level of an inviscid Burgers vortex and obtained $\Omega R_c^2/(V_0 R)=0.8829$ ($R_c/R=0.5$). This value corresponds to the critical swirl level of Benjamin[1] and will in the following be referred to as ω_B. A possible Reynolds number independence of the critical swirl level is indicated by a comparison with the two-dimensional axisymmetric and unsteady Navier-Stokes simulations of a swirling flow in a pipe by Lopez[7] at Re ≤ 1000, and the asymptotical method of Wang and Rusak[8] at Re=6000 (based on the pipe diameter). Lopez found that disturbances can propagate upstream only if $\Omega R_c^2 \geq 1.8$. According to the theory of Benjamin,[1] this value must correspond to the critical swirl level. If the value obtained by Lopez is nondimensionalized by the bulk velocity and the radius of the pipe ($V_0=1$ and $R=2$ in the work by Lopez), the critical swirl level predicted by Lopez is $\omega_B=0.9$, which is very close to the value obtained by Wang and Rusak.[9] Wang and Rusak[8] found a critical swirl level of $\omega_B=0.882\,864$ for a viscous vortex, a value more or less identical to the value obtained from their inviscid analysis. The quasicylindrical solution method derived herein predicts a critical swirl level of $\omega_B=0.8829$. It should be mentioned that the resemblance of the inviscid analysis of Wang and Rusak and the viscous simulations of Lopez[7] has earlier been verified by Wang and Rusak.[8,9] However, it is here shown that identical results can be obtained by an analysis of the quasicylindrical equations. A summary of the results are shown in Table I. The radial velocity for a Burgers vortex at Re=1000, as a function of the swirl number, S_c, is shown in Fig. 6. It is interesting to note that there are feasible solutions to the quasicylindrical approximation in the subcritical region [Fig. 6 (bottom)]. However, this vortex does not behave like the vortex in Sec. III A. The radial velocity is positive for all swirl levels lower than the first critical limit and it is negative in the slightly subcritical region. This also applies for all q vortices considered in this work. There is a sign change of the radial velocity component at the critical swirl level, which will lead to an acceleration of the axial flow in the subcritical region. This agrees with the two-dimensional analysis of unbounded vortices by Bossel.[13] In his analysis, $\partial_z V_z|_{r=0}$ changes sign from negative to positive as the swirl number is increased through the critical region.
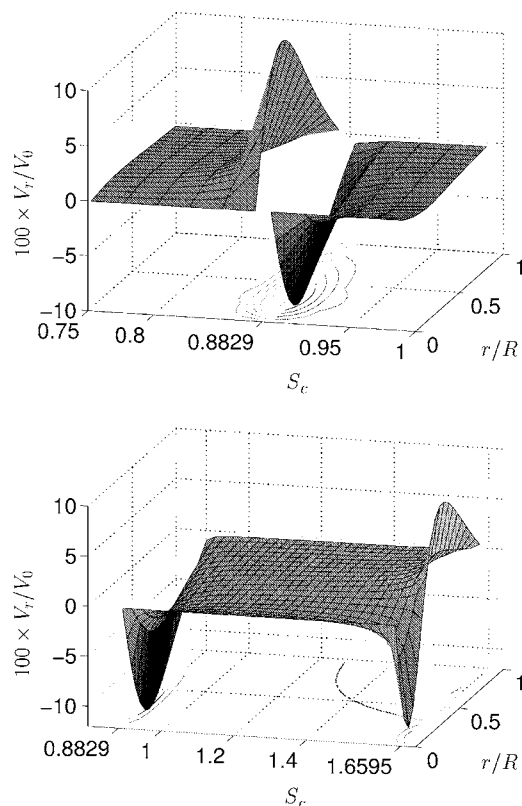
FIG. 6. The radial velocity component of a steady Burgers vortex around the critical swirl number, $S_{c,\text{crit}}$, computed from Eq. (14) at Re=1000. The swirl is varied by increasing coefficient Ω of Eq. (27). Top: The results violate the quasicylindrical assumptions in the near critical region because $100 \times V_r/V_0 \gtrsim 1$. Bottom: In narrow regions around the first and second critical swirl numbers, the results violate the quasicylindrical assumptions. The tendency of flow acceleration along the axis of symmetry appears in the entire subcritical region.

A second critical swirl level is found at $S_c=1.6595$. When the second singular point is crossed, the sign of $\partial_z V_z|_{r=0}$ will reverse again.

The radial velocity component at the inlet boundary is many times ignored in numerical simulations of swirling flow in a pipe; see, for example, Beran and Culick,[6] Brown and Lopez,[5] Lopez,[7] and Wang and Rusak.[4] However, the radial velocity component may be significant in the case of low Reynolds number flows. In fact, Eq. (14) suggests that it is inversely proportional to the Reynolds number. The constant of proportionality for a Burgers vortex with $R_c/R=0.5$ and a swirl level of $\Omega R_c^2/(V_0 R)=0.7305$, is 7.1, i.e., $\max(V_r)/V_0=7.1/\text{Re}$. This swirl level corresponds to the necessary condition for vortex breakdown as derived by Wang and Rusak[10] and shown by Lopez.[7] At Re$\lesssim 500$ (based on the pipe radius) the ratio $\max(V_r)/V_0 \sim 0.0142$, i.e., it is of the same order of magnitude as assumed in the derivation of the quasicylindrical approximation (see the Appendix). For very low Reynolds numbers, the method derived herein will not be applicable, at least not for an arbitrary vortex.

IV. CONCLUSIONS

A simple one-dimensional tool for determining the properties of an arbitrary vortex has been derived. In analogy with the inviscid theories of vortex breakdown, the present numerical analysis of quasicylindrical flows suggests that there is a critical level of swirl that may determine the point of vortex breakdown, i.e., where the quasicylindrical approximation fails to give a solution. This point is determined by the sign change of the smallest eigenvalue of matrix A in Eq. (21). It is shown that the critical swirl level obtained from the quasicylindrical approximation is identical to the sufficient condition for vortex breakdown as derived by Wang and Rusak[9] and Rusak et al.[10] The results also agree well with the studies of Lopez.[7] This may suggest that the critical swirl level of a swirling flow in a pipe is determined by the inlet boundary condition itself. In a narrow region around the critical swirl, the solutions to Eq. (14) are not consistent with the quasicylindrical assumptions unless the source term, Eqs. (18) or (19), vanishes. However, for swirl numbers higher than critical, the existence of quasicylindrical flow is again possible, at least in a time-averaged sense.

The critical level of swirl is not directly changed by either viscosity or turbulence. Instead, the effects of viscosity and turbulence will alter the critical level of swirl only by their influence on the shape of the mean axial and tangential velocity profiles. Numerical analysis of the equations that are derived in the present study allows a study of the properties of an arbitrary vortex. The major limitation of Eq. (14) is that only local properties of the vortex can be analyzed. However, by solving the equation for the radial velocity component of an arbitrary vortex, the continuity equation determines the near downstream behavior.

The determination of the radial velocity component for a steady viscous swirling flow requires knowledge of the axial and tangential velocity profiles only. In the turbulent or unsteady case, a proper model for the source term, Eq. (18), must be employed. An inverse relationship between the radial velocity and the Reynolds number is shown. At very low Reynolds numbers, no near columnar states exist for the vortices examined in this paper.

APPENDIX

1. Order of magnitude estimation

In "order-of-magnitude" estimates, equations governing a somewhat general swirling flow can be obtained, analogous to the derivation of the well-known boundary layer equations; see, for example, Schlichting.[25] Steenbergen[26] used the methodology to derive a set of equations for turbulent swirling flow, and here we follow a similar approach.

The time-averaged Navier-Stokes equations for an axisymmetric turbulent flow read

$$V_r \partial_r V_r + V_z \partial_z V_r - \frac{1}{r} V_\theta^2 = -\frac{1}{\rho} \partial_r P + \frac{1}{r} \partial_r (\nu r \partial_r V_r - r \overline{v_r' v_r'})$$
$$+ \partial_z (\nu \partial_z V_r - \overline{v_r' v_z'})$$
$$- \frac{1}{r} \left(\nu \frac{V_r}{r} - \overline{v_\theta' v_\theta'} \right), \tag{A1}$$

$$V_r \partial_r V_\theta + V_z \partial_z V_\theta + \frac{1}{r} V_r V_\theta = \frac{1}{r} \partial_r (\nu r \partial_r V_\theta - r \overline{v_r' v_\theta'})$$
$$+ \partial_z (\nu \partial_z V_\theta - \overline{v_\theta' v_z'})$$
$$- \frac{1}{r} \left(\nu \frac{V_\theta}{r} + \overline{v_r' v_\theta'} \right), \tag{A2}$$

$$V_r \partial_r V_z + V_z \partial_z V_z = -\frac{1}{\rho} \partial_z P + \frac{1}{r} \partial_r (\nu r \partial_r V_z - r \overline{v_r' v_z'})$$
$$+ \partial_z (\nu \partial_z V_z - \overline{v_z' v_z'}), \tag{A3}$$

and the corresponding continuity equation is

$$\frac{1}{r} \partial_r (r V_r) + \partial_z V_z = 0. \tag{A4}$$

The time-averaged equations follow directly from the instantaneous Navier-Stokes equations if the flow is decomposed as $v_i = V_i + v_i'$, where v_i' describes a fluctuation from the time-averaged velocity field, V_i. Gradients of viscosity are allowed in Eqs. (A1)–(A3) in order to facilitate the use of an eddy-viscosity closure for the unknown terms, $\overline{v_i' v_j'}$. The equations will look exactly the same for a steady flow, but all terms including turbulent fluctuations will vanish.

The order of magnitude of each term can be estimated by introducing a set of scaling parameters, U, u_t, L, and R. The velocity parameter, U, can be regarded as a typical velocity of the flow field and will scale $\{V_z, V_\theta\}$ in the Navier-Stokes equations. Hence, the axial and tangential velocities are considered to be of the same order of magnitude. Length parameters $\{L, R\}$ will scale $\{z, r\}$ and, while L must be regarded as the required length for a significant decay of swirl, R can simply be considered the radius of the vortex itself. For swirling flow in a pipe, R can be regarded as the radius of the pipe. The relations between the length parameters are assumed to be

$$\frac{L}{R} \gg 1. \tag{A5}$$

An estimate of the gradients will accordingly read

$$\partial_z \sim \frac{1}{L}, \quad \partial_z \partial_z \sim \frac{1}{L^2}, \quad \partial_r \sim \frac{1}{R}, \quad \partial_r \partial_r \sim \frac{1}{R^2}. \tag{A6}$$

By using the approximation of the gradients, Eq. (A6), the continuity equation (A4) will provide an estimate of V_r, i.e.,

$$V_r \sim \frac{UR}{L}. \tag{A7}$$

Assuming that an appropriate velocity scale for the turbulent fluctuations is $u_t < U$, the fluctuations can be estimated as $u_t \sim U \sqrt{R/L}$, i.e., one order of magnitude smaller than the mean velocity. This assumption is based on data from direct numerical simulations of turbulent channel flow by Moser *et al.*[27] and experimental data from turbulent swirling flow by Dellenback *et al.*[24] It follows that the magnitude of the terms in the steady axisymmetric Navier-Stokes equations (after normalizing by U^2/L) can be estimated as

$$\underbrace{V_r \partial_r V_r}_{\sim R/L} + \underbrace{V_z \partial_z V_r}_{\sim R/L} \underbrace{- \frac{1}{r} V_\theta^2}_{\sim L/R} = \underbrace{-\frac{1}{\rho} \partial_r P}_{\sim ?} + \underbrace{\frac{1}{r} \partial_r (\nu r \partial_r V_r)}_{\sim \mathrm{Re}^{-1}}$$
$$\underbrace{- \frac{1}{r} \partial_r (r \overline{v_r' v_r'})}_{\sim 1} + \underbrace{\partial_z (\nu \partial_z V_r)}_{\sim \mathrm{Re}^{-1} R^2/L^2}$$
$$\underbrace{- \partial_z (\overline{v_r' v_z'})}_{\sim R/L} \underbrace{- \frac{1}{r} \nu \frac{V_r}{r}}_{\sim \mathrm{Re}^{-1}} + \underbrace{\frac{1}{r} \overline{v_\theta' v_\theta'}}_{\sim 1}, \tag{A8}$$

$$\underbrace{V_r \partial_r V_\theta}_{\sim 1} + \underbrace{V_z \partial_z V_\theta}_{\sim 1} + \underbrace{\frac{1}{r} V_r V_\theta}_{\sim 1} = \underbrace{\frac{1}{r} \partial_r (\nu r \partial_r V_\theta)}_{\sim \mathrm{Re}^{-1} L/R} \underbrace{- \frac{1}{r} \partial_r (r \overline{v_r' v_\theta'})}_{\sim 1}$$
$$+ \underbrace{\partial_z (\nu \partial_z V_\theta)}_{\sim \mathrm{Re}^{-1} R/L} \underbrace{- \partial_z (\overline{v_\theta' v_z'})}_{\sim R/L}$$
$$\underbrace{- \frac{1}{r} \nu \frac{V_\theta}{r}}_{\sim \mathrm{Re}^{-1} L/R} \underbrace{- \frac{1}{r} (\overline{v_r' v_\theta'})}_{\sim 1}, \tag{A9}$$

$$\underbrace{V_r \partial_r V_z}_{\sim 1} + \underbrace{V_z \partial_z V_z}_{\sim 1} = \underbrace{-\frac{1}{\rho} \partial_z P}_{\sim ?} + \underbrace{\frac{1}{r} \partial_r (\nu r \partial_r V_z)}_{\sim \mathrm{Re}^{-1} L/R} \underbrace{- \frac{1}{r} \partial_r (r \overline{v_r' v_z'})}_{\sim 1}$$
$$+ \underbrace{\partial_z (\nu \partial_z V_z)}_{\sim \mathrm{Re}^{-1} R/L} \underbrace{- \partial_z (\overline{v_z' v_z'})}_{\sim R/L}. \tag{A10}$$

To a second-order accuracy, all terms of order $R/L \ll 1$ or smaller can be neglected. The Reynolds number of the flow is here defined as

$$\mathrm{Re} = UR/\nu. \tag{A11}$$

All terms including the viscosity are negligible when $\mathrm{Re} > 1000$ is chosen for the unsteady or turbulent case. On the other hand, if we choose to study a steady flow at $100 < \mathrm{Re} < 1000$, all terms including turbulent fluctuations will vanish and the viscous terms in the tangential and axial momentum equations (A9) and (A10) will remain, as they will reach the order of 0.1–1.

The only way for the right-hand side of the radial momentum equation (A8) to balance the left-hand side is for the pressure term to be of the order of L/R. This implies that the pressure must scale in the same way as the dynamic pressure, i.e.,

$$P \sim \rho U^2, \tag{A12}$$

and it follows that the pressure term of the axial momentum equation (A10) must be of the order of 1. Since the two remaining terms on the right-hand side of the radial momentum equation (A8) are two orders of magnitude smaller than the balance between the pressure term $(-\rho^{-1}\partial_r P)$ and the centrifugal force $(-r^{-1}V_\theta^2)$, they are negligible.

To a second order of accuracy, the time-averaged Navier-Stokes equations for turbulent swirling flow in a pipe read

$$-\frac{1}{r}V_\theta^2 = -\frac{1}{\rho}\partial_r P, \tag{A13}$$

$$V_r\partial_r V_\theta + V_z\partial_z V_\theta + \frac{1}{r}V_r V_\theta = -\frac{1}{r}\partial_r(\overline{rv_r'v_\theta'}) - \frac{1}{r}(\overline{v_r'v_\theta'}), \tag{A14}$$

$$V_r\partial_r V_z + V_z\partial_z V_z = -\frac{1}{\rho}\partial_z P - \frac{1}{r}\partial_r(\overline{rv_r'v_z'}), \tag{A15}$$

and, for steady flow $(100 < \mathrm{Re} < 1000)$, we have

$$-\frac{1}{r}V_\theta^2 = -\frac{1}{\rho}\partial_r P, \tag{A16}$$

$$V_r\partial_r V_\theta + V_z\partial_z V_\theta + \frac{1}{r}V_r V_\theta = \frac{1}{r}\partial_r(\nu r\partial_r V_\theta) - \frac{1}{r}\left(\nu\frac{V_\theta}{r}\right), \tag{A17}$$

$$V_r\partial_r V_z + V_z\partial_z V_z = -\frac{1}{\rho}\partial_z P + \frac{1}{r}\partial_r(\nu r\partial_r V_z). \tag{A18}$$

The latter equations are the quasicylindrical approximation used by Hall[12,22] and Bossel.[13–15] They constitute the basis for the estimation of the radial velocity component, if the two other components are given or measured in a single cross-sectional plane.

2. Numerical procedure

A finite volume method was chosen to solve Eq. (14). It can be rewritten as

$$\partial_r(f\partial_r V_r) + \partial_r((g - \partial_r f)V_r) + (h - \partial_r(g - \partial_r f))V_r = b, \tag{A19}$$

and integrated over small control volumes, Δr, to yield a linear discrete system of equations, i.e.,

$$A\mathbf{v} = \mathbf{s}. \tag{A20}$$

After including the boundary conditions (20) and using a second-order central difference scheme, we obtain a tridiagonal matrix in the form

$$A = \begin{bmatrix} a_{p,1} & a_{e,1} & 0 & \cdots & & \\ a_{w,2} & a_{p,2} & a_{e,2} & 0 & \cdots & \\ 0 & a_{w,3} & a_{p,3} & a_{e,3} & 0 & \cdots \\ \vdots & \ddots & \ddots & \ddots & \ddots & \ddots \end{bmatrix},$$

where the coefficients are

$$a_{e,i} = \frac{f_e}{\Delta r} + \frac{(g - \partial_r f)_e}{2},$$

$$a_{w,i} = \frac{f_w}{\Delta r} - \frac{(g - \partial_r f)_w}{2}, \tag{A21}$$

$$a_{p,i} = -\frac{f_w}{\Delta r} - \frac{f_e}{\Delta r} - \frac{(g - \partial_r f)_w}{2} + \frac{(g - \partial_r f)_e}{2} + (h - \partial_r(g - \partial_r f))_p\Delta r.$$

Subscripts e and w denote values at the east and west faces of each control volume, respectively, while subscript p denotes the value at the center. The discrete expression for the unknown radial velocity component is

$$\mathbf{v} = [V_{r,p,1}, V_{r,p,2}, \ldots]^T, \tag{A22}$$

and the integrated source term is simply

$$\mathbf{s} = [b_{p,1}, b_{p,2}, \ldots]^T\Delta r. \tag{A23}$$

The equation is solved for all $r_p = [\Delta r/2, 3\Delta r/2, \ldots, R - \Delta r/2]$ by Gaussian elimination.

Note that, in order to compute the coefficients of Eq. (14) in a proper way, the tangential and axial velocity profiles including their radial derivatives must be smooth and continuous.

[1] T. B. Benjamin, "Theory of the vortex breakdown phenomenon," J. Fluid Mech. **12**, 593 (1962).
[2] S. Leibovich and A. Kribus, "Large amplitude wavetrains and solitary waves in vortices," J. Fluid Mech. **216**, 459 (1990).
[3] A. Szeri and P. Holmes, "Nonlinear stability of axisymmetric swirling flows," Philos. Trans. R. Soc. London, Ser. A **326**, 327 (1988).
[4] S. Wang and Z. Rusak, "On the stability of an axisymmetric rotating flow in a pipe," Phys. Fluids **8**, 1007 (1996).
[5] G. L. Brown and J. M. Lopez, "Axisymmetric vortex breakdown. Part 2. Physical mechanisms," J. Fluid Mech. **221**, 553 (1990).
[6] P. S. Beran and F. E. C. Culick, "The role of non-uniqueness in the development of vortex breakdown in tubes," J. Fluid Mech. **242**, 491 (1992).
[7] J. M. Lopez, "On the bifurcation structure of axisymmetric vortex breakdown in a constricted pipe," Phys. Fluids **6**, 3683 (1994).
[8] S. Wang and Z. Rusak, "The effect of slight viscosity on a near-critical swirling flow in a pipe," Phys. Fluids **9**, 1914 (1997).
[9] S. Wang and Z. Rusak, "The dynamics of a swirling flow in a pipe and transition to axisymmetric vortex breakdown," J. Fluid Mech. **340**, 177 (1997).
[10] Z. Rusak, C. H. Whiting, and S. Wang, "Axisymmetric breakdown of a q-vortex in a pipe," AIAA J. **36**, 1848 (1998).
[11] Z. Rusak and K. P. Judd, "The stability of noncolumnar swirling flows in diverging streamtubes," Phys. Fluids **13**, 2835 (2001).
[12] M. G. Hall, "A new approach to vortex breakdown," in Proceedings of the Heat Transfer and Fluid Mechanics Institute, University of California, San Diego, La Jolla, CA, 1967, pp. 319–340.
[13] H. H. Bossel, "Vortex equations: Singularities, numerical solution, and axisymmetric vortex breakdown," NASA Contractor Report No. 2090, 1972, p. 74.
[14] H. H. Bossel, "Vortex breakdown flowfield," Phys. Fluids **12**, 498 (1969).
[15] H. H. Bossel, "Swirling flows in streamtubes of variable cross section," AIAA J. **11**, 1161 (1973).

[16]P. S. Beran, "The time-asymptotic behaviour of vortex breakdown in tubes," Comput. Fluids **23**, 913 (1994).

[17]T. W. Mattner, P. N. Joubert, and M. S. Chong, "Vortical flow. Part 1. Flow through a constant diameter pipe," J. Fluid Mech. **463**, 259 (2002).

[18]F. Sotiropoulos and Y. Ventikos, "The three-dimensional structure of confined swirling flows with vortex breakdown," J. Fluid Mech. **426**, 155 (2001).

[19]D. O. Snyder and R. E. Spall, "Numerical simulation of bubble-type vortex breakdown within a tube-and-vane apparatus," Phys. Fluids **12**, 603 (2000).

[20]T. Sarpkaya, "On stationary and travelling vortex breakdown," J. Fluid Mech. **45**, 545 (1971).

[21]S. V. Alekseenko, P. A. Kuibin, V. L. Okulov, and S. I. Shtork, "Helical vortices in swirl flow," J. Fluid Mech. **382**, 195 (1999).

[22]M. G. Hall, "Vortex breakdown," Annu. Rev. Fluid Mech. **4**, 189 (1972).

[23]V. Thome and S. Larsson, *Partial Differential Equations with Numerical Methods* (Department of Mathematics, Chalmers University of Technology, Gothenburg, 1999).

[24]P. A. Dellenback, D. E. Metzger, and G. P. Neitzel, "Measurements in turbulent swirling flow through an abrupt expansion," AIAA J. **26**, 669 (1987).

[25]H. Schlichting, *Boundary Layer Theory*, 7th ed. (McGraw-Hill, New York, 1979).

[26]W. Steenbergen, "Turbulent pipe flow with swirl," Ph.D. thesis, Eindhoven University of Technology, 1995.

[27]R. D. Moser, J. D. Kim, and N. N. Mansour, "Direct numerical simulation of turbulent channel flow up to $Re_\tau=590$," Phys. Fluids **11**, 943 (1999).